Caravaca II: Islands with Energy Storage: Inrush Current

Gonzalo Tejero Calvo, Student, *Universidad Pontificia de Comillas & University of Strathclyde*
August 2021

Abstract—In this paper, the islanding operation with energy storage is reviewed, with special focus on the inrush currents. The objective to reach a net zero emissions environment for 2050 is leading to the development of smart solutions to increase the number of green energy sources, which has led to the increase of the distributed generation. In this scene, a BESS island supposes a wide variety of benefits. However, it also implies several problems to be solved. Being one of these problems the inrush current phenomenon that take place whenever a feeder is connected due to the energization of the power transformers. An in-depth documentation analysis is made, followed by the development of several simulations to analyze the effects of the inrush current in the islanding operation. These simulations are contrasted with field experimentation at the Iberdrola BESS facility at Caravaca de la Cruz. Finally, three possible solutions are analyzed to overcome the inrush current issue.

Index Terms—Inrush Current, Transformer, Circuit Breaker, Battery, Voltage, Magnetic Flux, Feeder.

NOMENCLATURE

- BESS: Battery Energy Storage System
- B: Magnetic Flux Density [T]
- H: Magnetic Field Strength [A·t/m]
- PMU: Phasor Measurement Unit
- CB: Circuit Breaker

I. CONTEXT & JUSTIFICATION

With the huge increase of distributed generation in the power grid, mainly consisting of renewable power generation, the electric power system paradigm has changed. Traditionally, generation was situated far from consumption, connected by the power grid, based on transmission and distribution lines, which stablished a one-way power flow, from the generation at the top, to the consumers at the bottom of the electric power system. The development of renewable energy sources has made possible to situate generation closer to consumers, mainly in the distribution grid, therefore reducing transmission losses. Distributed generation raises some challenges. This project mainly focuses on one of these challenges, the generation of islands. Islanding takes place when a section of the power grid keeps energized even though the grid is supposed to disconnect due to a hazardous condition at the power grid. This event occurs in presence of a distributed generator in that section. Islanding keeps distribution lines and loads energized when they should be disconnected, therefore presenting two main problems. First, a dangerous situation can be raised for line and maintenance operators who count on a de-energized grid, and, secondly, if the reconnection to the power grid is carried out while the island has been operating independently, it may have gotten out of synchronization, therefore resulting in short-circuits that suppose a problem to the main grid.

However, islanding also implies that certain sections of the main power grid can operate as a microgrid, presenting some benefits listed below [1]:

- Microgrids increases the reliability of the grid by improving the continuity of the local power supply in case of contingencies in the electrical network, therefore improving the operation of the main power grid.
- Black-start restoration. In case of a black start, the presence of microgrid eases the restoration of the power grid, since microgrids can start operating independently from the network, and then, reconnect to the main grid.
- The integration of a Battery Energy Storage System (BESS) in the microgrid enable the addition of further services such as generation scheduling optimization, reactive power supply or voltage and frequency regulation, as well as imbalance compensation and spinning reserve operation. In addition, peak-shaving operation, optimization of wind and solar cycles and back-up system to the microgrid are also considered.

Although islanding operation is still prohibited, the clear advantages that it offers is boosting its investigation to solve the mentioned problems to benefit from the islanding mode of operation. Thus, Iberdrola has developed the Caravaca project, a BESS based microgrid to study and analyze the islanding operation mode. The battery supports the operation of four independent feeders.

When connecting and re-energizing each of the four feeders, huge current peaks appear, known as the inrush current. Inrush currents appear due to the magnetization of the transformers connected to the feeders. Basically, inrush currents can reach peak values of 12 times the nominal current and are generally extinguished in less than a second. The main problem with the inrush currents is that, although being an instantaneous phenomenon, it is seen as a fault by the electrical protections, which will open the CBs, hindering the feeder connection process.

Therefore, the main objective is to analyze the inrush currents phenomenon to obtain a precise simulation of the energization of a feeder to ensure the island operation mode.

II. Project Objectives

The main objective of this project is to study and analyze the inrush current phenomenon with the purpose of obtaining an accurate simulation capable of predicting the results for the energization of a feeder. If this objective if fulfilled, an estimation of the size of the feeders that can be energized by the battery without triggering protections can be done with the developed simulation. The completion of this objective is divided in 5 smaller objectives that are presented below:

- First, an in-depth analysis of the inrush current phenomenon is carried out including the transformer principles and operation.
- The second step of this project is to model a three-phase transformer that can emulate the energizing transient in addition to the steady-state operation. This simulation is carried out in Simulink. The special focus of this part of the project is to include the hysteresis and saturation B-H curve in the transformer model, which is the main cause of the elevated peak inrush current values. Several transformers are modelled with different parameters to obtain transformers with different power characteristics, with the objective of modelling and analyzing a real feeder.
- Thirdly, one of the four real feeders from the Caravaca facility is modeled. This simulation includes a wider number of elements to emulate the feeder as close as the reality as possible. The objective of this simulation is to analyze the operation of the feeder under different initial conditions to obtain an estimation of the inrush current value that appears when energizing the feeder. Additionally, an accurate estimation of the inrush current transient extinguishing times can be obtained. This simulation includes the protection installed at the Caravaca microgrid. Thus, it is possible to check if the connection of the simulated feeder triggers the electric protections.
- Fourthly, after all the required simulations have been carried out to analyze the connection of the feeder, a further analysis will be done in-site, where the results of the simulations will be compared to the real measures obtained from the Caravaca facility to analyze the accuracy of the model.
- Finally, and taking advantage of all the inrush current knowledge obtained through the whole project, an analysis of some possible solutions is made supported by the developed models to study the possible effects of each proposed solution.

III. State of the Art – Inrush Current

In this section, an in-depth analysis of the inrush current when energizing a transformer is made, for which, first, the fundamentals and operation of a transformer are reviewed.

The operation of a power transformer is mainly based on the electromagnetic induction, which is the process by which a changing magnetic field can induce a flowing current through a conductor.

The basic structure of a transformer is composed by two coils rolled around the same ferromagnetic core as shown in Figure 1.

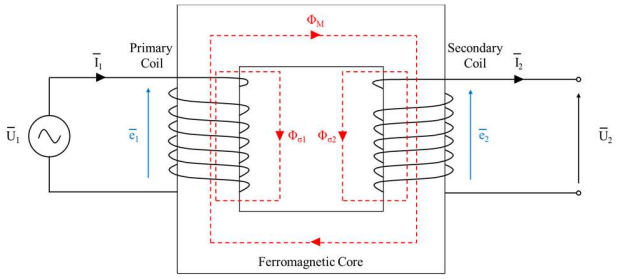

Figure 1. Basic structure of a single-phase transformer.

When an alternate voltage (U_1) is applied to the primary coil, an alternate current (I_1) flows through the coil, which establishes a magnetic flux (ϕ_M). The presence of the magnetic core facilitates a magnetic low reluctance path for the magnetic flux to link both primary and secondary coils. Following the Faraday and Lenz laws, the presence of a variable magnetic flux through the secondary coil, leads to the apparition of an electromotive force (e_2) that is going to oppose to the variation of the flux. Thus, the induced current (I_2) is obtained at the secondary coil. Additionally, the current flowing through both the primary and secondary coils is going to generate unwanted flux leakages represented by the dispersion flow through the air ($\phi_{\sigma1}$ and $\phi_{\sigma2}$), which produces an electromotive force in each coil ($e_{\sigma1}$ and $e_{\sigma2}$). The described operation of the transformer shown in Figure 1, is further analyzed by (1) and (2), where R1 and R2 correspond to the cupper losses in the primary and secondary coils, respectively.

$$U_1 = R_1 I_1 + e_{\sigma1} + e_1 \quad \textbf{(1)}$$

$$U_2 = e_2 - R_2 I_2 - e_{\sigma2} \quad \textbf{(2)}$$

Applying Faraday's Law to (1) and (2), (3) and (4) are obtained.

$$U_1 = R_1 I_1 + N_1 \frac{d\phi_M}{dt} + N_1 \frac{d\phi_{\sigma1}}{dt} \quad \textbf{(3)}$$

$$U_2 = N_2 \frac{d\phi_M}{dt} - R_2 I_2 - N_2 \frac{d\phi_{\sigma2}}{dt} \quad \textbf{(4)}$$

Finally, and assuming that dispersion fluxes are proportional to the current at normal load condition [1], (5) can be applied, where $L_{\sigma1}$ and $L_{\sigma2}$ are the equivalent inductances for the primary and secondary windings, respectively. Finally, (6) and (7) are obtained.

$$N \cdot \phi = L_\sigma \cdot I \quad \textbf{(5)}$$

$$U_1 = R_1 I_1 + N_1 \frac{d\phi_M}{dt} + L_{\sigma1} \frac{dI_1}{dt} \quad \textbf{(6)}$$

$$U_2 = N_2 \frac{d\phi_M}{dt} - R_2 I_2 - L_{\sigma2} \frac{dI_2}{dt} \quad \textbf{(7)}$$

On the other hand, if we apply the Ampere's law to the magnetic circuit presented in Figure 1, (8) is obtained.

$$N_1 I_1 - N_2 I_2 = \Re_m \phi_M \quad \textbf{(8)}$$

Rearranging (8), (9) is obtained.

$$I_1 = \frac{N_2}{N_1} I_2 + \frac{\Re_M \phi_M}{N_1} = \frac{N_2}{N_1} I_2 + I_M \qquad (9)$$

As seen in (9), the current flowing from the primary side can be divided in two terms, the current that is flowing to the secondary side, and the magnetic current, that is flowing through the magnetic core. This magnetic current is also going to produce some conduction losses on the iron core. However, the magnetic current is usually very low in comparison with the current flowing through the primary to the secondary side, so under normal conditions, it is usually neglected. With relation to the inrush current, it is important to highlight that, when no load is connected to the secondary side (being I_2=0), the current flowing through the primary side is going to be equal to the magnetic current.

The previous analysis of the transformer can be represented as an equivalent circuit following the equations presented above, and it is shown in Figure 2.

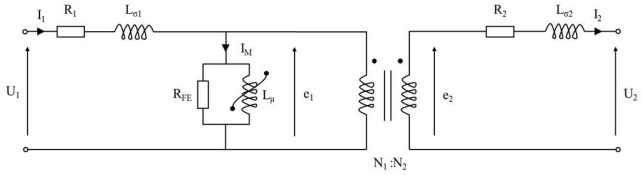

Figure 2. Equivalent circuit for a single-phase transformer.

In Figure 2, R_1 and R_2 represent the conduction losses at both primary and secondary windings. $L_{\sigma 1}$ and $L_{\sigma 2}$ correspond to the equivalent inductances that represent the effect of the flux leakage in both windings. The parallel branch corresponds to the effects of the magnetizing current. R_{FE} represent the conduction losses from the magnetic current at the iron core. L_μ is the equivalent to the magnetic circuit in charge of generating e_1. The superimposed parabolic line stands for the non-lineal nature of the magnetic core.

The relation shown in (10) between the B and H depends on the permeability of the core material (μ) [T·m/A], that is obtained from the relative permeability (μ_r) and the permeability of free space (μ_0), by (11).

Additionally, in (12), the relation between the magnetic flux (ϕ) and the magnetic flux density (B) is presented.

$$B = \mu \cdot H \qquad (10)$$

$$\mu = \mu_r \cdot \mu_0 \qquad (11)$$

$$\phi = B \cdot S \qquad (12)$$

In Figure 3 [2], the B-H curves for different core materials is presented.

While the B-H relation is constant for air cored magnets, for ferromagnetic cored magnets, the B-H relation is not constant. For those materials, the initial slope reaches a saturation point, from where the B-H relation is like the air-cored magnets.

Once the saturation point (a) is reached, if the magnetizing current that was generating the B is removed, the magnetic flux will not disappear completely, since the ferromagnetic core material will retain some of its magnetism (b). This phenomenon is known as residual magnetism (B_r) or residual flux (ϕ_r). It can be understood as some type of "memory". To remove this residual flux, a negative magnetizing current can be applied to the magnet (c), known as Coercive Force (H_c).

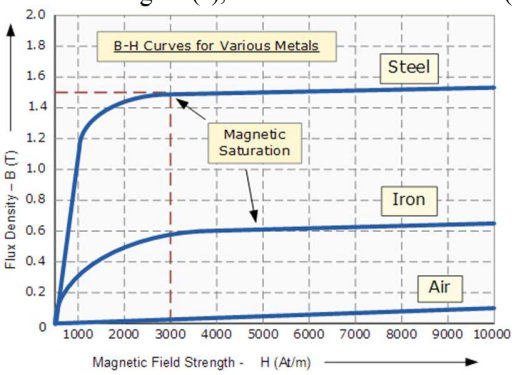

Figure 3. B-H curves for different core materials.

If this negative magnetizing current is increased further, the flux density will also increase in the reverse direction, reaching the reverse saturation point (d). If the magnetizing current is removed, the reverse residual point will be reached (e). In an AC system, the magnetic flux will constantly be varying though the positive and negative side of the curve, following the magnetic hysteresis loop, shown in Figure 4 [2].

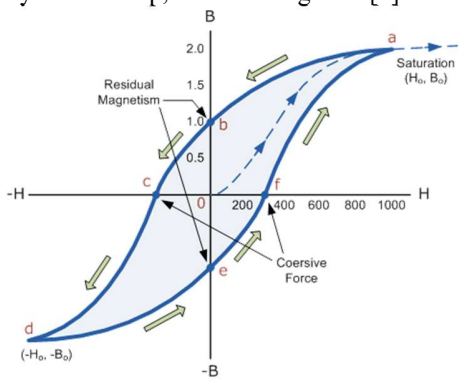

Figure 4. Hysteresis loop for a ferromagnetic transformer core.

Based on the Ampere law, H is directly related to the current flowing through the magnetic core, while B is directly related to the magnetic flux density of the magnetic core as seen in (12). This is the reason of the non-linear nature of the L_μ presented in Figure 2.

Once the main features of the transformer had been reviewed, the energization of the transformer going to be analyzed, since the connection of the transformer gives rises to the high-peak inrush current. To understand what happens when a transformer in energized, the following simplifications have been made:

- It is supposed that the transformer is energized with no load connected to the secondary side, therefore, no current flows through this side (I_2=0), and therefore both R_2 and $L_{\sigma 2}$ can be neglected.

- Supported by [3], both R_1 and $L_{\sigma 1}$, as well as R_{FE} have two main effects on the inrush current. First, R_{FE} represent the losses produced by the magnetizing current (I_M), therefore reducing the peak value of the inrush current, and secondly, R_1 and $L_{\sigma 1}$, have a damping effect on the inrush current. The inrush current is extinguished following a damping factor equal to $R_1/L_{\sigma 1}$. For an approximation to the problem, R_1 and $L_{\sigma 1}$ and R_{FE} are being neglected since it supposes the most unfavorable situation.

With the abovementioned simplifications, Figure 5 shows the resulting circuit.

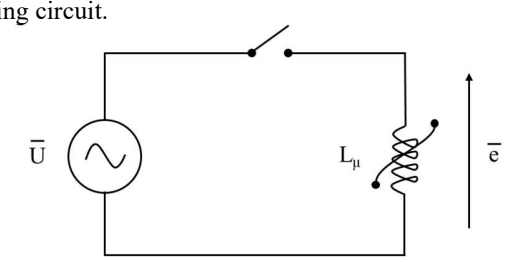

Figure 5. Analyzed transformer simplified circuit.

Considering U as an AC voltage source following a sinusoidal curve function of time (13), being U_p the peak voltage value, ω the angular frequency [2πf] and θ, in this case, being the angular point at which the switch is closed, and therefore the transformer energized.

$$U = U_p \cdot sin(\omega t + \theta) \quad \textbf{(13)}$$

In this simplified case, U=e. Applying the Faraday-Lenz law, (14) is obtained.

$$N_1 \frac{d\phi}{dt} = U_p \cdot sin(\omega t + \theta) \quad \textbf{(14)}$$

Rearranging (14) to obtain the value of the magnetic flux, (15) is obtained.

$$\phi = \frac{U_p}{N_1} \int \sin(\omega t + \theta) \cdot dt \quad \textbf{(15)}$$

Solving equation, the expression for the magnetic flux can be obtained (16), where the peak value for the flux is represented by (17).

$$\phi = -\phi_p \cdot \cos(\omega t + \theta) + \phi_t \quad \textbf{(16)}$$

$$\phi_p = \frac{U_p}{N_1 \omega} \quad \textbf{(17)}$$

As depicted by (16), the flux is delayed 90º with respect to the applied voltage that generates the flux. ϕ_t represents a transitory component of the magnetic flux, that appears at the connection of the transformer, and is the responsible of the high inrush current peaks. For the determination of the transitory term, it is crucial to look at the initial conditions. For the initial instant t=0, therefore obtaining (18), where ϕ_0 represents the residual flux and ϕ_{t0} represents the initial value for the transitory component of (16).

$$\phi_0 = -\phi_p \cdot cos\theta + \phi_{t0} \quad \textbf{(18)}$$

For the general case, where $\phi_0 = \phi_r$, (19) is obtained, representing the flux at the connection instant.

$$\phi = -\phi_p \cdot \cos(\omega t + \theta) + \phi_p \cdot cos\theta + \phi_r \quad \textbf{(19)}$$

In (19), it is shown that the flux generated at the energization of a transformer depends on the residual flux in the magnetic core, the voltage angle at which the transformer is energized, and the peak flux value, which, as seen in (17), is affected by the peak voltage value and the number of turns of the primary winding.

The worst-case scenario takes place when the magnetic core presents a residual flux ($\phi_r \neq 0$), and the transformer is energized when the voltage is equal to zero (θ = 0º). Under these conditions, the initial value for the transitory component is composed by the residual flux plus the peak flux value. As seen in Figure 6, the flux curve is vertically displaced a total value equal to ϕ_{t0}.

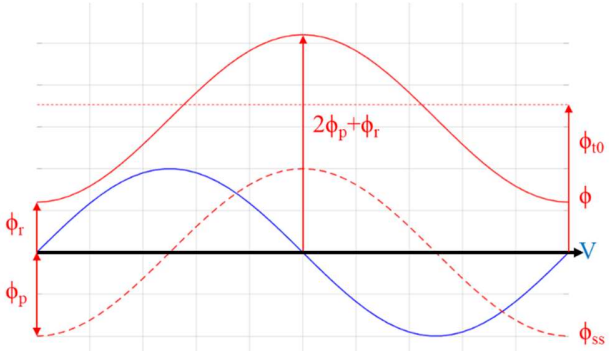

Figure 6. Worst-case scenario for the energization of a transformer, including the voltage (blue), the total flux (red), and the steady-state flux (stripped red).

In Figure 6, the vertical displacement due to the transformer being energized when the voltage is zero is represented by the ϕ_p, while the effect of the residual flux is shown by the ϕ_r. The flux reaches a peak of two times the flux peak in steady state plus the residual flux, therefore, at least doubling the total flux presented in the previous case.

In addition to the reached peak value, it is important to analyze the transient affecting the flux variation to know for how long these high peak values are maintained. As seen in (20), the flux expression is formed by a steady state and a transient term. The transient term is exponentially reduced following a damping factor that is related to the series impedance of the primary winding [3].

$$\phi = -\phi_p \cdot \cos(\omega t + \theta) + \left[\phi_p \cdot cos\theta + \phi_r\right] \cdot e^{\frac{-R_1}{L_{\sigma 1}}t} \quad \textbf{(20)}$$

As seen in Figure 7 [3], the total flux (ϕ_T) is composed by the steady-state flux (ϕ_{ss}), which is the sinusoidal part of the flux and a transitory term that is extinguished following the exponential function presented in (20). Therefore, the damping factor ($R_1/L_{\sigma 1}$) determines for how long the inrush effect is going to affect the system.

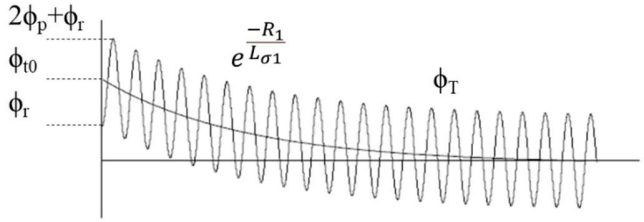

Figure 7. Total flux at the energization instant.

Once the flux has been determined, the current can be obtained thanks to the magnetizing B-H curve. Figure 8 [4] (a) presents the relation between the magnetizing current and the magnetic flux at the transformer core, which is an equivalent from the B-H curve of the ferromagnetic material. In Figure 8 [4] (b), the inrush current curve obtained from the total flux wave is shown. The high current peak is obtained from the saturation the flux-current curve presents. Under the saturation point, for a big

change in the magnetic flux, the current is going to present a slight change in its value. However, once the saturation point is reached, for each little increase in the flux value, a huge current increase appears. That is the reason for the high peak values of the inrush current.

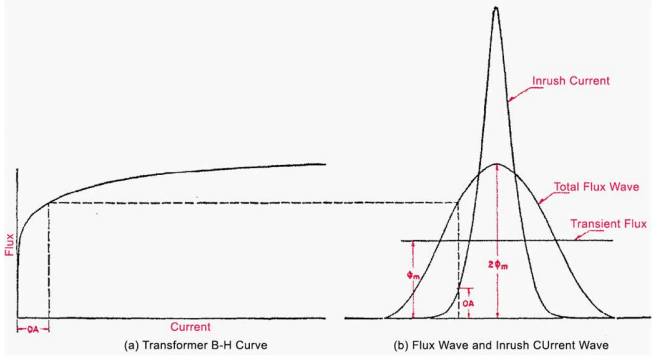

Figure 8. Transformer B-H curve.

A typical inrush current transient is shown in Figure 9 [3], where the inrush current peaks are all positive since the flux does not reach a zero value until the transient is almost fully extinguished.

Figure 9. Typical inrush current transient.

Finally, in [5], three different models for the non-linear ferromagnetic core are simulated, including:

- A linear resistance for R_{FE} and a non-linear inductor L_{μ}.
- A non-linear resistance for R_{FE} and a non-linear inductor L_{μ}.
- A linear resistance for R_{FE} and a non-linear inductor L_{μ} including the hysteresis loop.

The conclusions extracted from these three simulations are that the best results are obtained with the third model, although the first one being the simpler one.

IV. Simulations

A. Single Three-Phase Transformer

In this section, an analysis of a single three-phase transformer is made to verify the right operation of the simulation and the similarity to the theory presented in III.

The 50 kV transformer has been the chosen to study the energizing dynamic response, which parameters are obtained from [6].

The three-phase transformer included in the Specialized Power Systems section of the Simscape library from Simulink enables the possibility to include the hysteresis and saturation curves of the ferromagnetic core material required to emulate both the transient at the energization moment and the steady-state transformer operation.

The hysteresis and saturation curves are added to the model through a Matlab file generated thanks to the Powergui tool: "power_hysteresis". This tool enables the user to view and edit the hysteresis characteristic for a saturable transformer by defining:

- The remanent flux (Fr). The point which corresponds to the value that the flux takes when the current goes to zero.
- The coercive current (Ic). The value of the current when the flux is equal to zero. Additionally, the slope at this point is also required (dF/dI).
- And finally, the saturation point (Is, Fs) that indicates the point from which the ferromagnetic core material behaves as an air-cored material.

On the other hand, the saturation curve is also included in the Powergui tool, that it is introduced by the means of two equally-length vectors of current and flux values that define the saturation characteristic.

Before getting into more detail of how the saturation curve has been emulated, it is important to highlight the difference between the B-H and the flux-current curves. The B-H curve refers to the material used in the ferromagnetic transformer material, which depends on the sheet's width and the quality of the material. On the other hand, the flux-current curve depends on the transformer itself since the relation with the B-H curve depends on the magnetic core dimensions. The best approximation to the inrush current is therefore obtained by the electrical tests undertaken to the transformers.

The saturation characteristic had been adapted to match the maximum inrush current to the value that appears at the transformer datasheet [6].

In addition to the saturation and hysteresis curves, the windings connection, the initial fluxes, the nominal power and frequency, the magnetization resistance and both primary and secondary windings parameters are specified, including the nominal voltage, the series resistance and inductance.

The simulation, shown in Figure 10, consist of a single three-phase saturable transformer connected to a 400V BESS through a 400V/20kV transformer. In between both the three-phase CB and the distribution line (LA-56 conductor) can be found. Additional blocks are also included for the voltage, flux, and current measurements.

The simulation is previously initialized to stablish the residual fluxes at the power transformer. Thus, all simulations are preceded by an initialization process.

In this section, the effect of the variation of the line length on both the peak current value as well as the time it takes for the transient response to get extinguished is analyzed. For this purpose, three simulations are analyzed, including a 1 km, 10 km, and 50 km length distribution line.

Table I presents the results from these simulations.

Length (km)	1	10	50
Line peak voltage (pu)	1.413	1.408	1.370
Peak Flux (pu)	2.352	2.344	2.305
Phase Peak Current (pu)	14.856	14.700	14.038
Decreasing Time (s)	0.422	0.402	0.325

Table I. Line length variation simulation results.

With the line length increase, the voltage at the primary side of the transformer decreases due to the voltage drop at the distribution line.

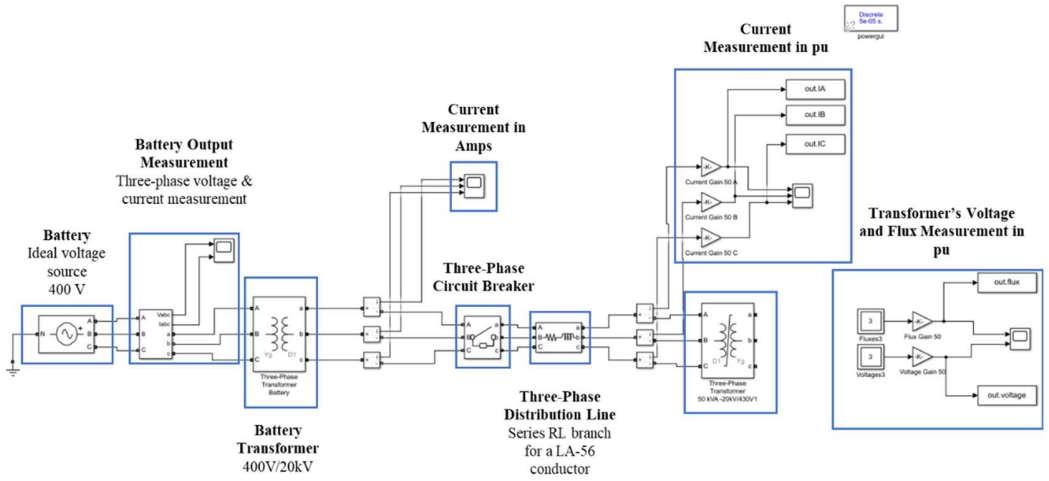

Figure 10. Simulink simulation scheme for a single three-phase transformer including the distribution line.

This results in a decrease of the peak flux value at the transformer, which, as previously discussed, is directly linked to the inrush current value. Therefore, the distribution line length increase, results in a peak current value reduction.

Additionally, it can also be checked that the distribution line length increase leads to a reduction in the time it takes for the current transient response to get extinguished qualitatively verifying the time constant presented in section III.

Results for the 1 km length distribution line are included in this paper to provide an idea of the dynamic response of the energization of a transformer. Figure 11 shows, from top to bottom, the line voltage at the primary side, the flux at the transformer, and the phase current flowing to the transformer, all in pu. In this first case, the voltage value is approximately equal to the nominal peak voltage value, the initial flux value is equal to the residual flux value reaching a peak value of up to 2.35 pu, which leads to a current peak value of almost 15 pu, which is the inrush current value presented in the transformer datasheet [6]. Figure 12, represents the transient response, where it can be checked that the inrush current phenomenon quickly decreases to get extinguished in 0.422 seconds.

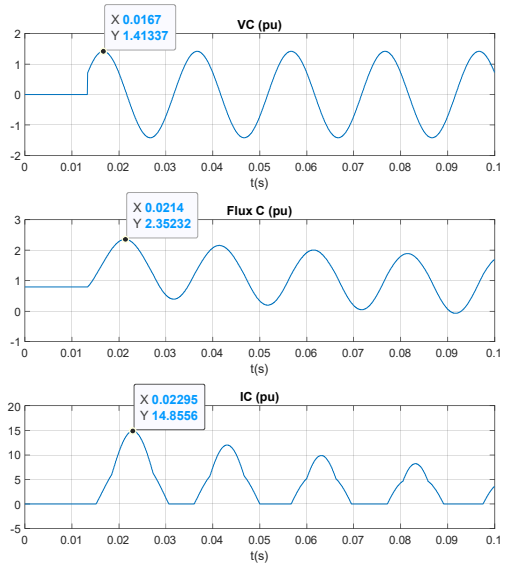

Figure 11. Dynamic energization response.

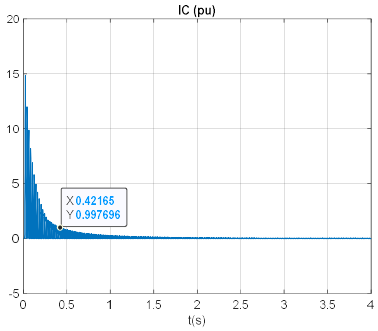

Figure 12. Transient energization response.

B. Feeder Simulation

In this section, a simulation of a real feeder from the Iberdrola BESS facility at Caravaca de la Cruz is built with the objective of analyzing the operation of a whole feeder.

Three main analyses are carried out. First, the effect of the voltage drops across the whole feeder is analyzed. Secondly, the voltage conditions that lead to each of the initial flux cases is simulated. Finally, the effect of the closing instant of the CB for different initial flux conditions is analyzed.

Figure 13 shows the single-line diagram of the emulated feeder. This feeder is composed by a sum of eight transformers, all connected by the respective distribution lines, and powered by a 400 V ideal source (battery equivalent) connected to the feeder by a 400V/20kV transformer. The distribution line lengths, as well as the nominal power for each transformer are depicted in the single-line diagram. CB at the top of this feeder, corresponds to a remote controlled three-phase CB. The nine red dots indicate the measurement points, where both the line voltages and phase currents are measured.

The objective of this first simulation is to see how the voltage drop across the feeder affects the inrush current of each transformer and the whole feeder.

For this purpose, measurements in the feeder include the line voltage at the primary side as well as the maximum inrush current value flowing to each transformer. The simulation is carried out to emulate the worst-case scenario, scilicet, when the inrush current value for each of the transformers forming the feeder reaches the highest possible value.

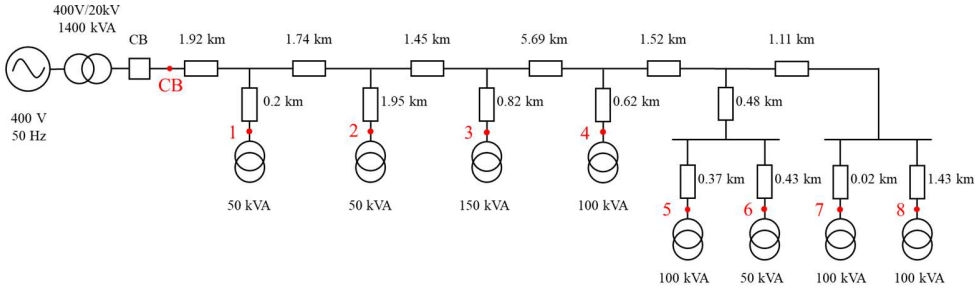

Figure 13. Single-line diagram for a real feeder from Iberdrola facility.

The measured inrush current is also compared to the maximum inrush current of each transformer, found at the transformer datasheet [6], to check the reduction for the inrush current value. Table II shows the results of the simulation.

As has been proved in previous sections, the inrush current is highly dependent on the voltage value through the means of the flux. The huge current values presented at the energization of the transformer leads to a huge decrease of the voltage at the primary side of the transformers because of the losses increase in the distribution lines. Therefore, the longer the distribution line connected to the transformer, the lower the voltage at the primary side when closing the CB, as can be observed from the results presented in Table II, by comparing, for instance point 1 with point 8. However, the temporary increase of the distribution losses causes a beneficial result for the feeder connection since the overall inrush current is decreased by a 24%. Finally, it is important to highlight that, the more downstream a transformer is in the distribution feeder, the higher the reduction of the inrush current.

In the simulations, it does not suppose a problem to look at the initial flux conditions, since it only requires setting a measurement in each transformer. However, measuring the initial flux conditions in a real feeder is much more complicated. Therefore, in the second simulation, the relation between the status of the voltage at the top of the feeder when opening the CB and the initial flux condition is going to be obtained.

For this simulation, the disconnection of all the transformers at the same time is considered since the disconnection is made with the CB at the top of the feeder. This leads to the same initial flux conditions for each of the transformers in the feeder, which is checked for each simulation. Twelve simulations, each corresponding to a 30º steps delay with respect to the instant at which the line voltage V_{ab} is positively crossing the zero value at the 20 kV side of the battery transformer, have been carried out for the described purpose.

Table III show the residual flux of each of the three phases (A, B and C) for each of the CB opening cases (in 30º steps). The residual flux value coincides with the residual flux nominal value. In each case, a positive, negative and zero residual flux values are presented. Six initial cases are obtained.

With these results, the initial flux conditions are matched to the voltage values at the 20 kV side of the battery transformer, being an easier measurement in real conditions.

Once the initial flux conditions are obtained, it is important to see the effects of closing the CB in different instants, therefore energizing the transformer for different voltage conditions.

With this purpose, for each of the analyzed 6 initial flux cases, 12 simulations had been carried out, by closing the CB in 30º delay steps. Results from these simulations are shown in Table IV. Each row corresponds to a different initial flux case, corresponding to the ones shown in Table III. Each of the columns corresponds to one of the 12 different CB closing instants. The dark-red colored cells represent the highest inrush current values matching with the worst-case scenarios for each case, while the dark-green colored cells represent the lowest inrush current values. The inrush current values range go from around 230 Amps, to nearly a zero current value.

From the results of these simulations, two main conclusions can be drowned. First, with the objective of minimizing the inrush current value, it is not possible to set a global instant to close the CB, since, depending on the initial flux condition, each of the closing instants is, at one or another initial case, close to a worst-case scenario. Furthermore, the worst-case scenario closing instant for one initial case, coincides with the best-case scenario for another initial case, where the inrush current phenomenon does not take place. Secondly, if we know the initial flux condition of the transformers at the feeder, it is possible to close the CB in an instant in which the inrush current effects are minimized and even removed.

Point	Description	Voltage (pu)	Estimated Current (A)	Measured Current (A)	Reduction (%)
1	Measurement of 50 kVA transformer	0.889	22	17.719	19.46%
2	Measurement of 50 kVA transformer	0.875	22	17.480	20.55%
3	Measurement of 150 kVA transformer	0.864	62	48.742	21.38%
4	Measurement of 100 kVA transformer	0.846	40	30.029	24.93%
5	Measurement of 100 kVA transformer	0.841	40	29.673	25.82%
6	Measurement of 50 kVA transformer	0.841	22	16.124	26.71%
7	Measurement of 100 kVA transformer	0.829	40	29.606	25.99%
8	Measurement of 100 kVA transformer	0.827	40	29.522	26.20%
CB	Measurement at the CB	0.902	288	219.070	23.93%

Table II. Simulation results for the voltage drop effect on the feeder

Steps		0º	30º	60º	90º	120º	150º	180º	210º	240º	270º	300º	330º
Initial Flux Condition	Flux A	-	0	0	+	+	+	+	0	0	-	-	-
	Flux B	0	-	-	-	-	0	0	+	+	+	+	0
	Flux C	+	+	+	0	0	-	-	-	-	0	0	+
Initial Case Nº		1	2	2	3	3	4	4	5	5	6	6	1

Table III. Initial flux condition at each phase for each of the CB opening cases.

		CB Triggering Steps											
		0º	30º	60º	90º	120º	150º	180º	210º	240º	270º	300º	330º
Initial Flux Condition	Case 1	30.941	0.314	27.497	85.181	139.190	159.287	197.952	219.070	203.876	153.424	137.280	87.820
	Case 2	141.481	91.810	31.261	0.307	28.356	84.094	140.043	159.451	201.937	223.718	208.175	159.246
	Case 3	212.963	164.240	141.336	90.387	30.335	0.293	29.248	90.925	145.057	165.057	207.445	228.950
	Case 4	207.896	228.536	213.285	163.351	135.118	85.960	23.944	0.298	34.328	96.577	150.288	170.530
	Case 5	149.937	169.269	200.800	222.945	207.914	159.057	131.473	81.365	25.606	0.318	34.103	94.512
	Case 6	33.972	88.617	142.794	163.455	197.965	219.437	203.537	154.124	132.718	81.600	25.681	0.312

Table IV. Inrush current maximum value in A for each of the initial flux condition and circuit closing case.

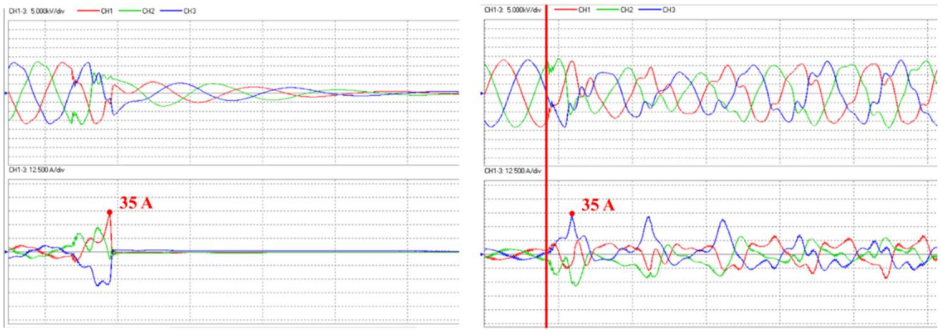

Figure 14. Voltage and current waveforms comparison for cases 1 (left) and 3 (right).

V. Field Tests

Seven different tests had been carried out that can be useful for the development of this thesis. All follow the same structure. In the first place, the system is operating in islanding mode with a determinate load that is going to be characterized by the total nominal load connected to the BESS. From this stable operating point, an additional feeder is connected to the BESS by closing a specific CB, which supposes the inclusion of an additional nominal power load to the system. Besides, the manufacturer of the BESS has implemented an algorithm based on the battery output voltage variation to improve the robustness of the islanding operation mode for the connection of feeders with a larger consumption.

In Table V, the seven tests are described, including the nominal power in kVA previously supported by the BESS system as well as the nominal power in kVA to be added through the CB closure. In addition, the status, active or inactive, of the BESS voltage-based algorithm and the number of repetitions of each test are presented.

Two main analyses can be differentiated. On the one hand, the first four cases are useful to give an overview of the inrush current phenomenon and a comparison of the effects of including the BESS inrush current algorithm. On the other hand, the last three cases are used to analyze if significant differences are presented if the CB is triggered at different instants.

No.	Previous Nominal Power Supported (kVA)	Nominal Power Addition (kVA)	Inrush Current Algorithm	Repetitions
1	2933	858	Inactive	1
2	1779	1154	Inactive	1
3	2933	858	Active	1
4	1779	1154	Active	1
5	2808	3230	Active	4
6	5342	696	Active	4
7	2708	4224	Active	5

Table V. Field tests description.

Figure 14 correspond to the comparison of cases 1 (left) and 3 (right), which include both the voltage (top) and current (bottom) waveforms for the three phases. The red line represents the moment in which the CB is triggered. The inrush phenomenon results in a huge current peak value. In this case, the presented results do not show the total peak current value since the system is disconnected before reaching its maximum current value or the control algorithm limits this value.

However, this current increase is depicted in the first four cases. It can be checked the relation between the voltage position at each phase and the reached peak current value at each phase, corresponding the maximum current value to the phase which voltage is at its minimum absolute value at the closing instant.

When the algorithm is not enabled, as the current provided by the battery reaches a certain limit value, the BESS shutdowns, the current falls instantly to zero, the voltage of the island quickly decreases till it reaches a zero value, and therefore, the whole system is de-energized. However, when the control algorithm is activated, as the current reaches this limit value, the voltage provided by the battery slightly decreases, therefore limiting the current value, supporting the connection of the added feeder.

The remaining 3 cases follow the same pattern. The connection of a different feeder in each case is repeated with the same system configuration, emulating the same operation for several times.

For each of the repetitions for each of the last three cases, the maximum current value had been measured, as shown in Table VI, through the event register that enables a further detailed analysis of the current and voltage waveforms when the event takes place.

		Repetition				
		1	2	3	4	5
Case	5	35	38.5	30	32.5	-
	6	32.5	33.75	35	36.25	-
	7	35	37.5	37.5	37.5	37.5

Table VI. Maximum inrush peak current values in A.

As seen from these results, for all cases, the reached peak current value is similar and close to 35 A in general. This consecutive reached value is a consequence of the activation of the voltage control algorithm, which allows the connection of larger feeders to the system without triggering the battery protections. However, for the purpose of this thesis, applying this control to the system leads to a loss of information, since the current is limited and therefore presents very similar values for all cases.

VI. Possible Solutions

In this section, three possible solutions are discussed.

A. PMU

This first solution comes from a conclusion drawn from Table IV, where it has been proved that the inrush current value is highly dependent of a combination of the initial flux condition and the CB closing instant.

If the residual flux at each phase is known before closing the CB, the effects of the inrush currents can be minimized, even removed when energizing the transformers. As seen in Table III, a direct relation between the remaining residual flux and the voltage status at the opening of the CB can be stated. Therefore, this first solution consists in the installation of a device capable of precisely registering the voltage signal at the opening and closing instants.

A PMU, also known as synchrophasor can be used for this purpose. A PMU generates a three-phase phasor by sampling voltage and current measurements acquired using the respective transformers. The generated voltage and current phasors are a representation of the magnitude and phase angles of the sampled waveform in the complex plane.

Several commercial PMU are integrated with detection and protection devices such as protection relays, CB, and timers [7].

Using a PMU, the most efficient connection and energization of the island could be performed by first registering the voltage status when the island is disconnected and therefore de-energized, and secondly, and thanks to the use of a PMU integrated CB, by closing the CB at the instant that minimizes the inrush effects. Furthermore, this process could be automatized to optimize the CB closing depending on the registered initial flux case, being an overall effective method to reduce the inrush current value or even remove it.

B. Single-Phase CBs

The best-case scenario for the energization of a transformer takes place when the voltage at the primary side is at its maximum absolute value since the flux will be at its minimum value. The main problem when considering a three-phase transformer is that, since it is powered through a three-phase balanced system, the voltage at each of the three phases is delayed 120º in respect to each other. Thus, the closing of the CB when the voltage is at its maximum value at each phase is not possible.

However, in this section, the possibility of changing the three-phase CB for three single-phase CBs is analyzed. The main objective of this change is to determine if the independent closure of each phase can reduce the overall inrush current value for the six different flux initial cases.

The important point of this solution is that it would not require a previous knowledge of the initial flux condition of the feeder. Instead, the three single-phase CBs would be always closed at the same instant, when the voltage at each phase reaches its highest absolute value.

Table VII shows the comparison between the use of a single three-phase CB and the use of three single-phase CBs for the 6 possible initial flux cases. Results show that there is an overall reduction of the maximum inrush current values, moving from a maximum current peak of up to 15.2 pu to a maximum inrush current value of up to 7.6 pu.

For a better understanding of this current reduction, Figure 15 is presented, where the three-step connection leads to a voltage and, thus, a flux reduction which ends in the current reduction.

	Case 1	Case 2	Case 3	Case 4	Case 5	Case 6
Imax Three-Phase CB (pu)	0.016	6.172	10.934	15.253	10.996	5.864
Imax Single-Phase CB (pu)	0.015	3.905	6.895	7.61	5.737	4.975
Reduction (%)	6.25	36.73	36.94	50.11	47.83	15.16

Table VII. Inrush current maximum value comparison.

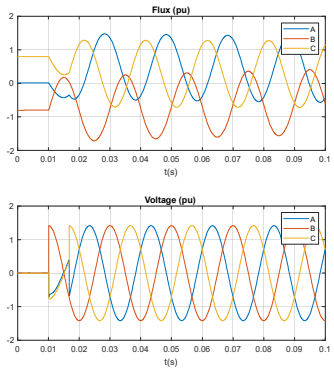

Figure 15. Single-phase CBs simulation voltage & flux.

The main outcome from this solution is that the independent triggering of each CB results in a voltage reduction in the first energization instants that leads to a flux reduction, which corresponds to an overall reduction of around 50% of the inrush current value.

C. Voltage Variation

This last proposal is focused on the voltage variation of the BESS when energizing a transformer.

Two main cases can be discussed. If the system is totally disconnected and the energization is done from a zero-voltage value, the ideal way to carry out this voltage variation is to implement a voltage ramp from a zero value to the nominal voltage value. However, when the system is in normal operation and an additional transformer is to be added to the system, the voltage value cannot fall below a certain value. Following the Spanish network code [8], the undervoltage limitation is set to a decrease of 15% in the voltage amplitude maintained for, at most, 1.5 seconds, which sets the simulation parameters.

The results of programming the voltage ramp from a zero-voltage value to its nominal value results in the reduction of the magnetic flux, which reaches a maximum value of 1.35 pu, as shown in Figure 16, leading to a maximum current value of 1.27 pu, thus representing a 90% reduction of the current value.

However, when programming a voltage ramp starting from 0.85 pu to its nominal value when energizing a transformer, the reduction is not so significant, resulting in a 20% reduction.

Based on these conclusions, the optimal way to energize a whole island system composed by several feeders would be all at once, since the zero to nominal value ramp could be implemented. If some other feeder had to be connected, the inrush current reduction effects are not as straight forward as for this first case.

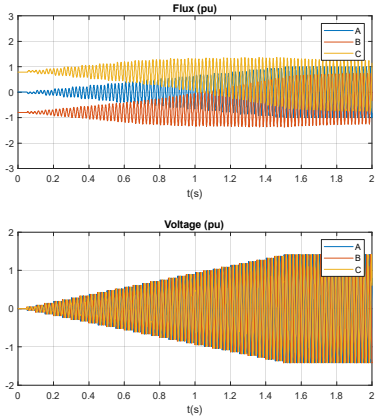

Figure 16. Ramp implementation simulation results.

To implement this solution, the voltage variation could be included in the inverter control by programming the voltage reference value to follow the required voltage ramp.

VII. Conclusions

Five main conclusions can be drawn from this thesis.

- First, through the combination of the offered tools both in Matlab and Simulink, the simulation of a transformer capable of reproducing the dynamic response that the energization of a feeder supposes has been achieved. The inclusion of the effect of the magnetizing characteristics of the transformer, which includes both the hysteresis and saturation curves, had been successfully achieved, which are the main causes for the inrush current apparition.
- An analysis of the transformers response when energized has been carried out. With this analysis, it can be verified that the transformers operation truly reproduces the inrush current behavior that has been reviewed in the investigation section of this project.
- Thirdly, the successful emulation of a real feeder has been achieved, obtaining an accurate estimation of the reached inrush current value that is produced when energizing a set of transformers connected by the distribution network. Besides, a precise inrush current estimation could be done for feeders with different configurations if needed.
- The simulation results show that it is possible to determine the initial flux status of the transformers of a feeder by keeping a voltage status register. Then, and knowing this initial status, it would be possible to trigger the circuit breaker in the optimum instant that could lead to the removal of the inrush current issue.
- The strong relation between the inrush current value and the voltage status at the connection instant has been proved both by the developed simulations and the field carried out experimental tests.

References

[1] J. Rocabert, A. Luna, F. Blaabjerg and P. Rodríguez, "Control of Power Converters in AC Microgrids," in IEEE Transactions on Power Electronics, vol. 27, no. 11, pp. 4734-4749, Nov. 2012.

[2] Magnetic Hysteresis Loop including the B-H curve. Electronics Tutorials. URL: https://www.electronics-tutorials.ws/electromagnetism/magnetic-hysteresis.html

[3] S.V. Kulkarni, S.A. Khaparde. Inrush Current in Transformer Engineering. Design, Technology, and Diagnostics (Second Edition, pp. 11-20). CRC Press.

[4] Westinghouse Electric Corporation. XIV. Exciting and Inrush Currents in Electrical Transmission and Distribution Reference Book (Fourth Edition, pp. 124-130).

[5] Amir Tokić, Ivo Uglešić, Gorazd Štumberger, "Simulations of Transformer Inrush Current by Using BDF-Based Numerical Methods", Mathematical Problems in Engineering, vol. 2013, Article ID 215647, 10 pages, 2013.

[6] Construcciones Eléctricas Jara, "Transformadores de distribución MT/BT – Especificación Técnica", TP-50/24/20 B2-O-PA.

[7] Ersan Kabalci, Yasin Kabalci, "Chapter 1 - Introduction to smart grid and internet of energy systems", in Smart Grid to Internet of Energy, pp. 1-62, 2019.

[8] Real Decreto 647/2020, de 7 de julio, por el que se regulan aspectos necesarios para la implementación de los códigos de red de conexión de determinadas instalaciones eléctricas. July 2020. Ministerio para la Transición Ecológica y el Reto Demográfico. Spain.